HAL
open science

Physical properties of YB66 and consideration of possible use for high-resolution X-ray optics

D Bessas, H Fukui, K Sugimoto, K Glazyrin, I Sergueev, G Levchenko, A Dukhnenko, V Filipov, O Isnard, D Ishikawa, et al.

To cite this version:

D Bessas, H Fukui, K Sugimoto, K Glazyrin, I Sergueev, et al.. Physical properties of YB66 and consideration of possible use for high-resolution X-ray optics. Journal of Applied Physics, 2021, 130 (2), pp.025105. 10.1063/5.0054482 . hal-04158353

HAL Id: hal-04158353

https://hal.science/hal-04158353v1

Submitted on 11 Jul 2023

HAL is a multi-disciplinary open access archive for the deposit and dissemination of scientific research documents, whether they are published or not. The documents may come from teaching and research institutions in France or abroad, or from public or private research centers.

L'archive ouverte pluridisciplinaire **HAL**, est destinée au dépôt et à la diffusion de documents scientifiques de niveau recherche, publiés ou non, émanant des établissements d'enseignement et de recherche français ou étrangers, des laboratoires publics ou privés.

Journal of Applied Physics ARTICLE scitation.org/journal/jap

Physical properties of YB_{66} and consideration of possible use for high-resolution X-ray optics

Cite as: J. Appl. Phys. **130**, 025105 (2021); doi: 10.1063/5.0054482
Submitted: 19 April 2021 · Accepted: 23 June 2021 ·
Published Online: 12 July 2021

View Online Export Citation CrossMark

D. Bessas,[1,a)] H. Fukui,[2,3] K. Sugimoto,[4] K. Glazyrin,[5] I. Sergueev,[5] G. Levchenko,[6] A. Dukhnenko,[6] V. Filipov,[6] O. Isnard,[7] D. Ishikawa,[3,4] H. Yoshikawa,[8] O. Sakata,[9] and A. Q. R. Baron[3]

AFFILIATIONS

[1]ESRF - The European Synchrotron, F-38043 Grenoble, France
[2]Graduate School of Material Science, University of Hyogo, 3-2-1 Kouto, Kamigori 678-1297, Hyogo, Japan
[3]Materials Dynamics Laboratory, RIKEN SPring-8 Center, Sayo-gun, Hyogo 679-5148, Japan
[4]Japan Synchrotron Radiation Research Institute (JASRI), 1-1-1 Kouto, Sayo-cho, Sayo-gun, Hyogo 679-5198, Japan
[5]Deutsches Elektronen-Synchrotron, D-22607 Hamburg, Germany
[6]Institute for problems of material science NASU, Krzhyzhanovsky 3, U-03142 Kyiv, Ukraine
[7]Université Grenoble Alpes/Institut Néel, CNRS, rue de Martyrs, B.P. 166, F-38042 Grenoble, France
[8]National Institute for Materials Science, Semgen 1-2-1, Tsukuba, Ibaraki 305-0047, Japan
[9]Synchroron X-ray group and Synchrotron X-ray station at SPring-8, National Institute for Materials Science, Sayo-gun, Hyogo 679-5148, Japan

[a)]**Visitor at:** Materials Dynamics Laboratory, RIKEN SPring-8 Center, Sayo-gun, Hyogo 679-5148, Japan.
Author to whom correspondence should be addressed: bessas@esrf.fr

11 July 2023 08:07:10

ABSTRACT

A combined microscopic, i.e., powder and single crystal x-ray diffraction and inelastic x-ray scattering, and macroscopic, i.e., heat capacity, characterization was carried out on YB_{66} between 10 and 400 K. The system crystallizes in a rather large unit cell with a lattice parameter of about 23.4 Å at room temperature. The volume thermal expansion coefficient is found to be $3.9 \times 10^{-5}\,K^{-1}$ at 295 K. A high Debye temperature above 1000 K was determined using several methods, 1043(25) K, from heat capacity measurements, 1430(59) K, from elastic constants measurements, and 1690(198) K, from thermal expansion measurements. The thermal transport is modeled as a collection of Einstein oscillators with an Einstein temperature of 194(2) K. The C_{11} and C_{44} elastic constants are above 400 and 150 GPa, respectively. The average speed of sound in YB_{66} is estimated to be 9631(380) m/s, similar to the average speed of sound in corundum, 10 000 m/s. The large volume of the unit cell and the stiffness of the crystal structure make YB_{66} a promising candidate for high-resolution x-ray monochromatization applications. Candidate reflections for high-resolution resonant inelastic x-ray scattering are indicated and potential pitfalls relevant to the quality of crystals and multi-beam cases are mentioned.

Published under an exclusive license by AIP Publishing. https://doi.org/10.1063/5.0054482

I. INTRODUCTION

Resonant inelastic scattering is a powerful tool to obtain element specific properties of a physical system.[1] Close to a resonance the scattering cross section maximizes and otherwise hidden elemental properties may come up. A high degree of monochromatization combined with high flux is the basic requirement in resonant inelastic scattering techniques for resolving collective excitations, such as phonons or magnons, in condensed matter.

A challenge in obtaining high energy resolution in x-ray scattering is directly related to the high energy, E, of the x-ray beam, which typically falls in the range between a few keV and several dozens keV. This practically indicates that in order to obtain an energy bandpass, δE, in the meV or sub-meV range, which is the pertinent energy scale for phonons and magnons, a relative energy resolution $\delta E/E$ between 10^{-7} and 10^{-9} is required.

The monochromatization of x rays is typically realized through high Miller indice reflections from single-crystalline solids.[2] A well

Published under an exclusive license by AIP Publishing

known approach to increase the degree of monochromatization and at the same time to increase the angular acceptance is by reflecting x rays in backscattering geometry. The relative energy resolution, $\delta E/E$, is directly proportional to the spread, δd, of the interatomic distance, d, over the full illuminated area of the crystal. Thus, in order to obtain a high degree of monochromatization, a tight tolerance in $\delta d/d$ and consequently in the quality of the crystal across the volume of single-crystalline solid is set. Provided a reflection in backscattering geometry exists the fine energy scanning may only be realized by varying the temperature and consequently the interatomic distance, d, of the material used as a monochromator. Thus, the knowledge of the thermal expansion coefficient for a system to be used as a high-resolution backscattering monochromator is important.

A high degree of monochromatization is difficult to be obtained in the case of resonant inelastic x-ray scattering applications. This is because reflections at a well defined energy can scarcely be found to match the backscattering geometry. The current paradigm for increasing the density of reflections for x-ray backscattering monochromatization applications is limited to the use of low symmetry crystals. Solids that crystallize in a low symmetry unit cell, e.g., SiO_2[3] or Al_2O_3,[4] tend to form a large volume unit cell and have a high density of x-ray reflections, whereas solids that crystallize in a high symmetry unit cell, e.g., Si, tend to form a small volume unit cell and have a low density of x-ray reflections. The knowledge and practical experience on the growth of bulk single crystals with a low symmetry unit cell, such as Al_2O_3, is still hampered from the uncontrolled appearance of various kinds of defects, dislocations, and twinning[5] that deteriorate notably the crystal quality and the obtained energy resolution.

An additional dimension in x-ray monochromatization is the stiffness of the crystal structure. The stiffer the crystal structure, the higher the reflected x-ray intensity.[6] Important to note is that the low stiffness imposes strong limitations for using SiO_2 in applications that require high energy-resolution monochromatization.[3,7,8]

The volume of the unit cell, the stiffness of the crystal structure, the thermal expansion coefficient, and the crystal quality constitute the quad for high-resolution x-ray monochromatization applications.

In this study, we explore the potential of using YB_{66}[9–12] as a backscattering monochromator. We thoroughly characterize using both microscopic (i.e., powder and single crystal x-ray diffraction, and inelastic x-ray scattering) and macroscopic experimental techniques (i.e., calorimetry) YB_{66} samples that crystallizes in a large cubic symmetry unit cell (space group: $Fm\bar{3}c$). We suggest reflections appropriate for high-resolution resonant inelastic scattering and we propose high symmetry large unit cell crystals such as YB_{66} for high-resolution x-ray monochromatization applications.

II. EXPERIMENTAL TECHNIQUES

A. Samples

Two types of YB_{66} samples were used in this study.

An YB_{66} single crystal was grown at IPMS NASU, Kyiv by a crucible free inductive zone melting with the specialized equipment "Crystal-111" under pure argon overpressure as described in Refs. 11, 13, and 14. The purity of initial components (Y_2O_3 and amorphous boron) was 99.994% and 99.9%, respectively. The main impurities in amorphous boron are O, H, and C. Oxygen, hydrogen, and carbon are effectively removed during the process of borothermal reduction in vacuum. The remaining impurities are removed during zone refining. The powders were cold pressed into rods and sintered under vacuum for an hour at 1800 °C. Pre-sintered rods were used for single crystal growth. The main difficulty for YB_{66} crystal growth is related to the fact that its electrical conductivity reaches admissible values only at the melting temperature. This makes it impossible to heat this material inductively. In order to circumvent this issue, we used an yttrium dodecaboride crystal as a starting seed to heat effectively the initial rod. Several passes through the inductor were applied in order to melt the full rod. The grown YB_{66} crystals had a length between 20 and 30 mm and a diameter between 6 and 8 mm. Each obtained rod consisted of a single-crystalline core (between 4 and 6 mm diameter) surrounded by a polycrystalline periphery with thickness between 1 and 2 mm. The polycrystalline outer layer was removed mechanically and the single crystalline core was used for further research. Pieces from this sample growth were crushed and x-ray diffraction and calorimetry measurements were carried out.

Pieces from an YB_{66} commercially produced (Crystal Systems Inc) high quality single crystal were studied using single crystal x-ray diffraction and inelastic x-ray scattering. The obtained pieces were cut from a $10 \times 20 \times 1\,mm^3$ single crystal used for long time as a monochromator at BL15XU at SPring 8.[9] We note that the crystal quality of this material was significantly better in terms of having high reflectivity from high index Bragg reflections.

B. X-ray diffraction

The powder x-ray diffraction measurements were carried out at P02.2 beamline at PETRAIII, DESY, Hamburg, Germany. The sample used was a powderized YB_{66} single crystal from the one grown at IPMS NASU, Kyiv. In order to get an extended Q-range and thus to record more reflections the energy of the incoming x-ray beam was set to 42.8 keV (wavelength: 0.29 Å). The x-ray beam was focused down to 3 μm horizontally and 8 μm vertically. The powder sample had a thickness around 100 μm; thus, between 10 and 100 crystallites were illuminated by the x-ray beam. The powder x-ray diffraction measurements were carried out in transmission geometry. We utilized a cold finger cryostat and a Perkin-Elmer XRD1621 detector for obtaining temperature dependent x-ray diffraction patterns between 10 and 300 K. The powder x-ray diffraction patterns of all recorded reflections were refined using JANA2006.

The single crystal x-ray diffraction measurements were carried out at BL02B1 beamline at SPring-8 in Japan on the sample obtained from BL15XU. The energy of the incoming x-ray beam was set to 29.95 keV (wavelength: 0.4139 Å). The single crystal x-ray diffraction measurements were carried out in transmission geometry. In order to obtain a large number of reflections ω(angle)-scans were carried out during the measurements. We utilized a XR-HR10K-S cryofurnace (Japan Thermal Engineering Co. Ltd.) and an PILATUS3 X CdTe 1M detector (Dectris) for obtaining temperature dependent x-ray diffraction patterns between 200 and 400 K. The single crystal x-ray diffraction patterns were refined and the lattice

11 July 2023 08:07:10

Published under an exclusive license by AIP Publishing

parameter of YB_{66} at different temperatures was extracted using CrysAlis^{Pro} (Rigaku Co.).

C. Calorimetry

The heat capacity at constant pressure, C_P, is measured between 10 and 250 K using the relaxation technique[15] by utilizing the calorimeter embedded in the Quantum Design Physical Property Measurement System (QD-PPMS). The sample used for the calorimetry measurements was a fragment of 13.3 mg with at least one flat surface obtained from the single crystalline aggregate sample grown at IPMS NASU, Kyiv.

The calorimetry measurements were carried out at the same temperature points first on the calorimeter platform loaded with a small amount of apiezon N grease and after with the sample embedded in the apiezon N grease loaded on the calorimeter platform. The heat capacity at constant pressure, C_P, of the sample was extracted by subtracting the heat capacity of the calorimeter platform with the apiezon N grease from the heat capacity of the sample embedded in the apiezon N grease loaded on the calorimeter platform. Each measurement was carried out three times. An average value and an errorbar were extracted and given in this study. Heat capacity measurements between 250 and 300 K were not carried out in order to avoid a known irregular contribution in the heat capacity relevant to apiezon N grease.[16]

D. Inelastic x-ray scattering

The inelastic x-ray scattering measurements[17,18] were carried out at the BL43LXU beamline[19] of SPring-8 in Japan on the sample obtained from BL15XU. The energy of the incoming x rays was set to 21.747 keV (wavelength: 0.5701 Å). The Si (11 11 11) analyzers reflection was used. The provided energy resolution was about 1.3 meV as extracted from the recorded elastic scattering of polymethyl methacrylate (PMMA) at room temperature. The YB_{66} sample was located in the vacuum chamber of a He cold finger closed-cycle cryostat with possibility to vary the temperature between 10 K and room temperature. The inelastic x-ray scattering spectra on YB_{66} were recorded around the (16 0 0) reflection. X-ray inelastic energy scans between −15 and 15 meV were carried out around the elastic line and the dispersion of both the longitudinal and the transverse acoustic phonons across (1 0 0) and (1 1 0) was recorded between 100 and 300 K.

III. RESULTS

The diffraction patterns of both the powder and the single crystalline YB_{66} samples at all temperatures are free from spurious reflections that might indicate impurity phases. No reflection splitting was identified in the full temperature range that might indicate a structural phase transition.

After refining the obtained powder and single crystal x-ray diffraction patterns, the lattice parameter, a, of YB_{66} between 10 and 400 K is obtained and shown in Fig. 1. The lattice parameter of YB_{66} shows a monotonous increase in the measured temperature range. A theoretical model suitable for simple crystallographic systems based on the Debye approximation[20] was used to fit the lattice parameter data. The theoretical model used for fitting the experimentally

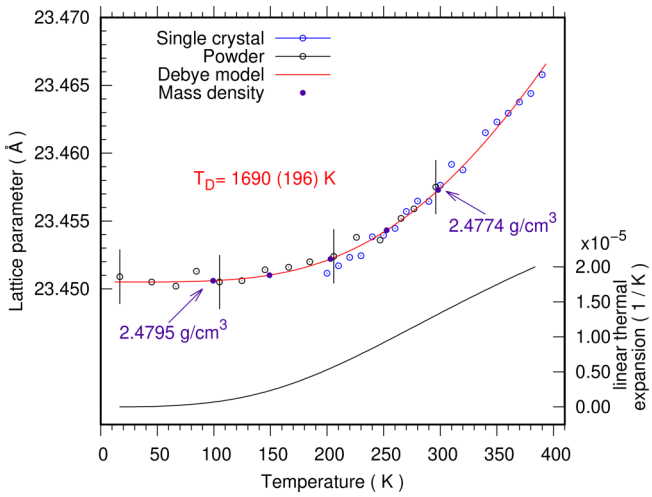

FIG. 1. The lattice parameter of YB_{66} extracted from x-ray diffraction measurements carried out on a powder sample (black points); see the text; between 15 and 300 K and on a single crystal (blue points) carried out between 200 and 400 K. A fit of the lattice parameter between 15 and 400 K using a Debye model (see the text) is depicted with a red line. Typical errorbars for the lattice parameters obtained using x-ray diffraction by powder samples are given. The errorbars in the lattice parameters obtained using x-ray diffraction by single crystalline samples do not exceed the pointsize. The calculated linear thermal expansion coefficient (see the text) of YB_{66} is depicted in the lower portion of the figure.

obtained lattice parameters is summarized in the formula

$$a(T) \approx a_0 + I_a T f(t),$$

where a_0 is the lattice parameter of the unit cell at 0 K, I_a is a function of compressibility and Grüneisen parameter, $f(t) = \frac{3}{t^3}\int_0^t \frac{x^3}{e^x-1}\,dx$ with $t = \Theta_D/T$, Θ_D is the Debye temperature, and T is the temperature of the sample.

The theoretically obtained curve for the temperature dependence of the lattice parameter is also shown in Fig. 1. The extracted lattice parameter of the unit cell at 0 K is $a_0 = 23.4505(2)$ Å, $I_a = 2.5(5)\times10^{-4}$ Å/K, and the extracted Debye temperature is 1690(196) K. Using the theoretically obtained curve for the lattice parameter, the linear thermal expansion coefficient, $\alpha_a = \frac{da(T)/dT}{a(T)}$, is calculated and is also included in Fig. 1. The volume thermal expansion coefficient, α_V, of the unit cell is simply $\alpha_V = 3\alpha_a$ and at 295 K is 3.9×10^{-5} K^{-1}.

The absence of a phase transition in YB_{66} is also confirmed from calorimetry measurements. A smooth heat capacity curve is obtained from the calorimetry measurements carried out between 10 and 250 K shown in Fig. 2. The heat capacity experimental data points were fitted using a Debye model, C_{Deb}, superimposed with a collection of Einstein oscillators, C_{Ein},[21] and the typical electronic contribution to heat capacity, γT, for metals. The fit of the model to the experimental data points is also seen in Fig. 2. The fit is rather satisfactory both in the high temperature regime and in the low temperature regime, shown as inset of Fig. 2. The extracted Debye temperature is 1043(25) K. The obtained Einstein

11 July 2023 08:07:10

Published under an exclusive license by AIP Publishing

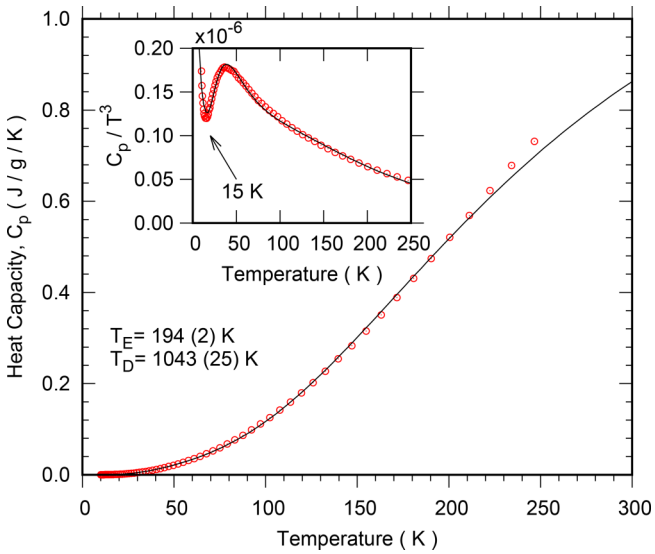

FIG. 2. The heat capacity at a constant pressure (red points) measured on a polycrystalline fragment of YB_{66} between 10 and 250 K and a fit of the experimental points (black line) using a Debye model including an ensemble of Einstein oscillators and the electronic contribution to heat capacity; see the text. Inset: The same data are shown in the Debye representation, C_p/T^3, with emphasis in the low temperature regime. The errorbars do not exceed the area of the data points.

temperature is 194(2) K. The coefficient, γ, for the electronic contribution to heat capacity is $5.8(3)\times10^{-6}$ J/(g K^2).

Typical inelastic x-ray scattering spectra at (0.15 0 0) and (0.25 0 0) measured on YB_{66} at room temperature are shown in Fig. 3. The phonon creation and the phonon annihilation side of the phonon spectrum on YB_{66} are clearly seen. The linear dispersion of the longitudinal acoustic phonon along (1 0 0) in YB_{66} is indicated in Fig. 3. Similar inelastic x-ray scattering spectra were measured for both longitudinal and transverse polarization phonon modes in the studied temperature range. The obtained inelastic scattering spectra were fitted with a sum of pseudo-Voigt profiles, a convolution of a Lorentzian profile relevant to the measured phonon mode, and a Gaussian profile relevant to the instrumental function and the crystallinity of the sample. The mixing ratio η of the Lorentzian and the Gaussian profile in the used pseudo-Voigt profiles was set to 0.5. The extracted energy, E in meV, of the phonon modes at the measured phonon momentum, Q in nm^{-1}, and the polarization and the direction of propagation at all temperatures are given in Table I.

The phonon group velocity, υ in m/s, is extracted by fitting the two experimental points shown in Table I per vibrational polarization at all propagation directions using the formula

$$E(\text{meV}) = 6.582\times10^{-4}\times\upsilon(\text{m/s})\times Q(\text{nm}^{-1}).$$

Notably, the formula used in this study for extracting the phonon group velocity is a linear function between energy and momentum.

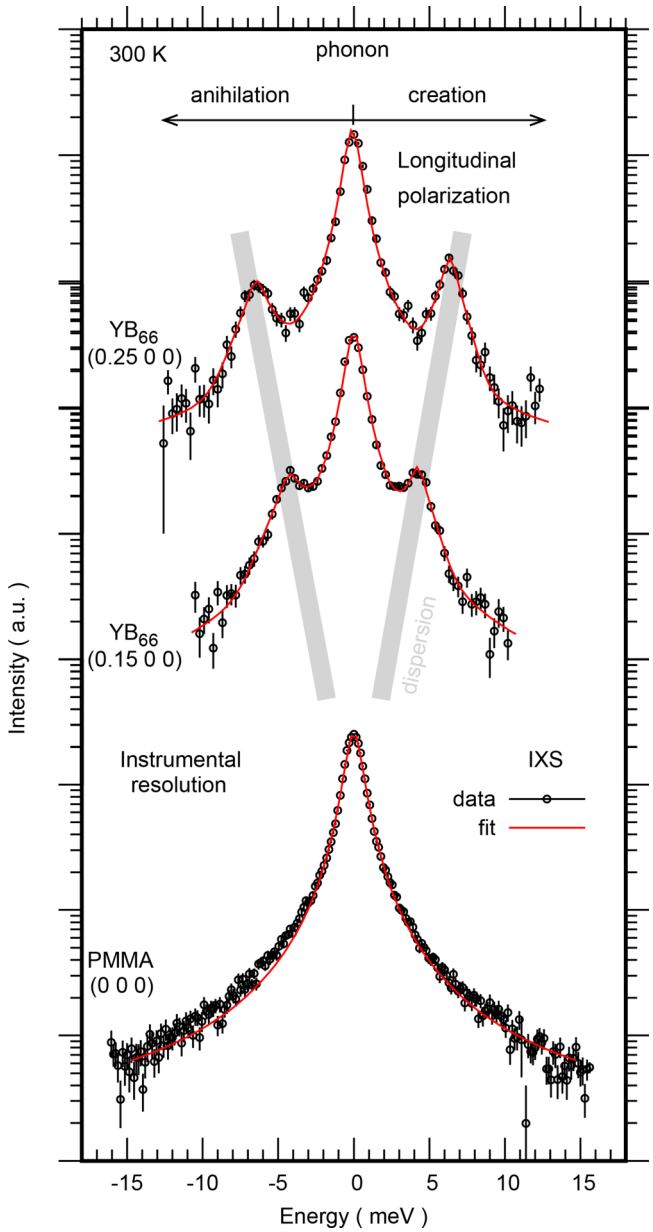

FIG. 3. Inelastic x-ray scattering (IXS) spectra (black points) measured on YB_{66} around the (16 0 0) reflection at room temperature and a fit (see the text) of the spectra (red line). The dispersion of a longitudinal acoustic phonon both in the phonon creation and in the phonon annihilation part of the spectrum is indicated. The instrumental function of the spectrometer (see the text) is shown in the lower portion of the figure by the PMMA spectrum. The experimental data at different momentum transfers are shifted vertically proportionally to the momentum change for clarity.

The curvature of the phonon dispersion curve at low energies is assumed negligible.

The calculated longitudinal and transverse phonon group velocities along (1 0 0) and (1 1 0) are shown in Fig. 4.

11 July 2023 08:07:10

Published under an exclusive license by AIP Publishing

TABLE I. Summary of the acoustic phonon mode parameters of YB_{66} explored in this study using inelastic X-ray scattering.

T(K)	Direction	Polarization	E (meV)	Q (nm^{-1})
100	(1 0 0)	Long.	3.63 (13)	0.40 (1)
			5.98 (9)	0.67 (1)
		Trans.	4.48 (26)	0.80 (1)
			5.82 (25)	1.07 (1)
	(1 1 0)	Long.	6.39 (43)	0.76 (1)
			9.63 (18)	1.14 (1)
		Trans.	4.36 (14)	0.76 (1)
			6.38 (9)	1.14 (1)
150	(1 0 0)	Long.	3.74 (15)	0.40 (1)
			5.84 (8)	0.67 (1)
		Trans.	4.48 (24)	0.80 (1)
			5.82 (13)	1.07 (1)
	(1 1 0)	Long.	6.28 (23)	0.76 (1)
			9.33 (27)	1.14 (1)
		Trans.	4.21 (12)	0.76 (1)
			6.42 (12)	1.14 (1)
200	(1 0 0)	Long.	3.48 (12)	0.40 (1)
			5.81 (8)	0.67 (1)
		Trans.	4.50 (21)	0.80 (1)
			5.84 (14)	1.07 (1)
	(1 1 0)	Long.	6.41 (17)	0.76 (1)
			9.48 (21)	1.14 (1)
		Trans.	4.25 (8)	0.76 (1)
			6.35 (9)	1.14 (1)
250	(1 0 0)	Long.	3.46 (7)	0.40 (1)
			5.80 (7)	0.67 (1)
		Trans.	4.35 (14)	0.80 (1)
			5.79 (13)	1.07 (1)
	(1 1 0)	Long.	6.17 (26)	0.76 (1)
			…	…
		Trans.	4.16 (8)	0.76 (1)
			…	…
300	(1 0 0)	Long.	4.24 (6)	0.50 (1)
			6.35 (6)	0.76 (1)
		Trans.	3.73 (14)	0.68 (1)
			5.01 (11)	0.94 (1)
	(1 1 0)	Long.	7.68 (21)	0.96 (1)
			11.08 (20)	1.33 (1)
		Trans.	5.24 (7)	0.96 (1)
			7.28 (6)	1.33 (1)

The longitudinal phonon group velocities across both (1 0 0) and (1 1 0) are above 12 km/s, whereas the transverse phonon group velocities are above 8 km/s for all measured temperatures. An increase in all phonon group velocities at lower temperature is observed.

Two irreducible elastic constants for a cubic structure C_{11} and C_{44} are extracted from the measured phonon group velocities using the formulas $C_{11} = \rho[v_{LA}(100)]^2$ and $C_{44} = \rho[v_{TA}(100)]^2$, where ρ is the mass density.[22] Assuming that the mass density is kept equal to the mass density at room temperature, 2.477 g/cm^3, the extracted elastic constants C_{11} and C_{44} of YB_{66} between 100 and 300 K are given in Fig. 4.

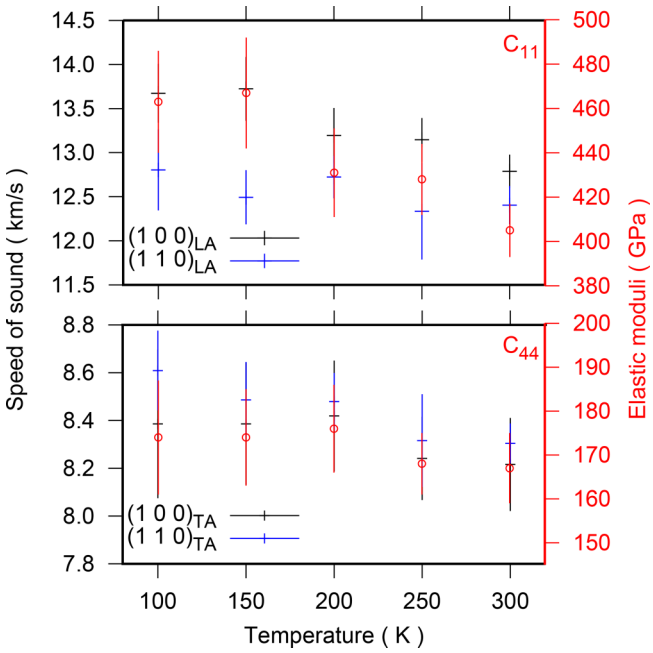

FIG. 4. (left panels) The temperature dependence of the longitudinal acoustic (upper portion) and the transverse acoustic (lower portion) speed of sound across the (1 0 0) and the (1 1 0) directions in YB_{66} extracted from IXS measurements. (right panels) The elastic moduli extracted (see the text) from the speed of sound measurements of the left panel.

IV. DISCUSSION

A. Physical properties

YB_{66} was first discovered in 1958 by Seybolt[23] during a study of boron-rich yttrium alloys. Initially, because of the low yttrium content, it was difficult to establish a precise formula for the compound.[24] Its range of composition was found to be limited to only 1–2 at.% yttrium. X-ray diffraction explored its crystal structure[25] and later the crystal structure of YB_{66} was established precisely.[26] Among the impressive characteristics of YB_{66} is the quite large unit cell, with a lattice parameter of 23.4 Å at room temperature, that includes 1584 boron and 24 yttrium atoms.

Little is known about the thermal expansion coefficient of YB_{66}. Only a single study on thermal expansion coefficient of YB_{66} could be found in the literature[27] using dilatometry on a rather large sample ($\sim 6 \times 6 \times 15$ mm^3) of YB_{66}. In this study, the thermal expansion coefficient of YB_{66} is extracted from x-ray diffraction measurements between 10 and 400 K. At room temperature, the volume thermal expansion coefficient in this study is found to be 3.9×10^{-5} K^{-1}, which is a typical thermal expansion coefficient for metals.[28] In Ref. 27, the volume thermal expansion coefficient of YB_{66} at room temperature is estimated to be 1.2×10^{-5} K^{-1}.

11 July 2023 08:07:10

Published under an exclusive license by AIP Publishing

There is a discrepancy between the thermal expansion coefficient of YB_{66} presented in this study and in Ref. 27. We could not find any information in Ref. 27 about the accuracy and precision of the dilatometer used to measure the thermal expansion coefficient of YB_{66}; thus, a further discussion is excluded.

The metallic behavior of YB_{66} close to room temperature is confirmed also by the heat capacity measurements carried out in the context of this study. The theoretical model for the heat capacity fails to describe the data if an electronic contribution to specific heat is not included. The electronic contribution to specific heat is found to be $5.8(3)\times10^{-6}\,\mathrm{J/(g\,K^2)}$. The same heat capacity data indicate the presence of a collection of local vibrational modes with an Einstein temperature of 194(2) K that is expected to deteriorate the lattice thermal conductivity. Thus, the phonon glass–electron crystal behavior[29] attributed to YB_{66} may be fully justified from our heat capacity measurements.

The elasticity of YB_{66} is not fully explored in the literature. According to Ref. 30, assuming elastic isotropy (absence of C_{12}) the values for C_{11} and C_{44} are reported to be $3.8\times10^9\,\mathrm{N/m^2}$ (or 3.8 GPa) and $1.66\times10^9\,\mathrm{N/m^2}$ (or 1.66 GPa), respectively. Such literature values are very low for an otherwise stiff solid, and by two orders of magnitude different from the corresponding values reported herein, i.e., $C_{11} = 405(12)$ GPa and $C_{44} = 167(8)$ GPa, at room temperature. Since it is not clear how the elastic constants are measured in Ref. 30, a further discussion cannot be justified.

In this study, using high-resolution inelastic x-ray scattering, we were able to extract the phonon group velocities across (1 0 0) and (1 1 0) in both longitudinal and transverse polarization of the acoustic dispersion branches. Although C_{11} and C_{44} are extracted directly from the measured group velocities $\upsilon_{LA}(100)$ and $\upsilon_{TA}(100)$, this is not the case for C_{12}, which is a combination of C_{11}, C_{44}, and $\upsilon_{LA}(110)$, where $C_{12} = 2(\rho[\upsilon_{LA}(110)]^2 - C_{44}) - C_{11}$. Only a temperature averaged $\overline{C}_{12}$ is extracted in this study and found to be $\overline{C}_{12} = -2(24)$ GPa. A probable reason for the arguably low temperature averaged value of C_{12} might be related with the high stiffness of YB_{66}.

From the obtained elastic constants, an average speed of sound, u_m, in YB_{66} can be extracted. The average speed of sound, $3/u_\mathrm{m}^3 = 1/u_\mathrm{p}^3 + 2/u_\mathrm{s}^3$, is calculated via $u_\mathrm{p} = \sqrt{\frac{K+(4/3)G}{\rho}}$ and $u_\mathrm{s} = \sqrt{\frac{G}{\rho}}$, where $K = \frac{C_{11}+2C_{12}}{2}$ and $G = \frac{G_\mathrm{V}+G_\mathrm{R}}{2}$ with $G_\mathrm{V} = \frac{C_{11}-C_{12}+3C_{44}}{5}$ and $G_\mathrm{R} = \frac{5C_{44}(C_{11}-C_{12})}{3C_{11}-3C_{12}+4C_{44}}$. For simplicity, here we use the temperature averaged elastic constants $\overline{C}_{11} = 439(9)$ GPa, $\overline{C}_{12} = -2(24)$ GPa, and $\overline{C}_{44} = 172(4)$ GPa extracted from the elastic constants measured at different temperatures in the temperature region studied herein. After doing the algebra, $K = 218(24)$ GPa, $G_\mathrm{V} = 191(9)$ GPa, $G_\mathrm{R} = 189(20)$ GPa, and $G = 190(15)$GPa. Thus, $u_\mathrm{p} = 13\,794(629)$ m/s, $u_\mathrm{s} = 8758(339)$ m/s, and $u_\mathrm{m} = 9631(380)$ m/s. The average speed of sound in YB_{66}, 9631(380) m/s, is quite high and directly comparable with the average tabulated speed of sound in corundum, i.e., 10 000 m/s.

The heat capacity close to room temperature is away from the Dulong–Petit limit. This observation is in agreement with the rather high Debye temperature, 1043(25) K, extracted from fitting the heat capacity data with a theoretical model. The Debye temperature extracted from the thermal expansion measurements is also quite high, 1690(198) K. A Debye temperature, T_D, can also be extracted from the measured average speed of sound, u_m, using the formula[21] $_\mathrm{D} = \frac{\hbar}{k_\mathrm{B}}(6\pi^2 N)^{1/3} u_\mathrm{m}$, where $\hbar = h/2\pi$ is the Planck constant, k_B is the Boltzmann constant, $N = \rho N_\mathrm{A}/\overline{M}$ is the atomic density, ρ is the mass density, N_A is the Avogadro constant, and $\overline{M}$ is the mean atomic mass. The mean atomic mass of YB_{66} is 11.97 g/mol. The mass density at room temperature is $2.477\,\mathrm{g/cm^3}$; thus, the atomic density of YB_{66} is $N = 1.24\times10^{23}\,\mathrm{atoms/cm^3}$. The calculated Debye temperature from the measured elastic constants, 1430(59) K, is also rather high.

The Debye temperature extracted in this study from heat capacity measurements, 1043(25) K, from elastic constants measurements, 1430(59) K, and from thermal expansion measurements, 1690(196) K, span into a large temperature range. Discrepancies in the extracted Debye temperature based on microscopic and macroscopic experimental techniques are expected. This is mainly related to the energy region of the vibrational spectra that is probed in the inelastic scattering spectra, the temperature region relative to the Debye temperature where the heat capacity measurements were carried out,[31] and the description of the phonon contribution to thermal expansion.[20]

B. X-ray optics

YB_{66} is not a new system for the x-ray optics community. Several decades after its first discovery, the synchrotron radiation community realized that YB_{66}, with its large interplane distance, $d = 0.586$ nm, for the (4 0 0) reflection can be used as a double crystal monochromator for dispersing synchrotron radiation below

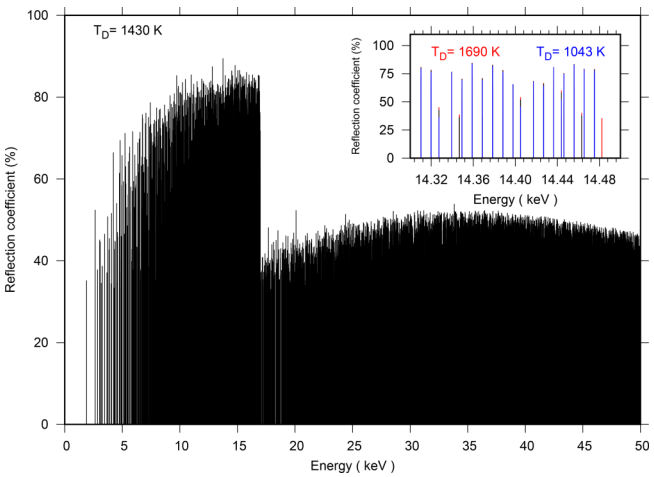

FIG. 5. Bragg backscattering reflections calculated for an YB_{66} single crystal at 295 K with x-ray energy between 1 and 50 keV and a reflection coefficient more than 33%. Calculations are performed by the dynamical theory of diffraction for a single crystal of infinite thickness. A Debye temperature of 1430 K (black lines) was used for all atoms in the unit cell (see the text). The jump in the reflectivity at *ca.* 17 keV is indicative of the Y x-ray absorption K-edge. Inset shows in an expanded view reflections with a reflection coefficient more than 33% at an x-ray energy between 14.3 and 14.5 keV for a Debye temperature of 1043 K (blue lines), 1430 K (black lines), and 1690 K (red lines).

11 July 2023 08:07:10

Published under an exclusive license by AIP Publishing

TABLE II. The theoretically expected energy bandpass (δE), the angular acceptance at exact backscattering ($\delta\Theta$), the resolving power (δE/E), the extinction length (Ext.), and the peak reflection coefficient (Refl.) of x rays for a given backscattering reflection of perfect YB_{66} at temperature T that can be used to carry out x-ray spectroscopy around an x-ray absorption edge. The Debye temperature of the perfect YB_{66} crystal is taken to be 1430 K.

X-ray edge	Energy (keV)	Reflection ($h\ k\ l$)	δE (meV)	$\delta\Theta$ (μrad)	δE/E 10^{-7}	Ext. (μm)	Refl. (%)	T (K)
Mn-K	6.539	(4 20 14)	4.7	99	7.2	49	32	234
Fe-K	7.112	(18 0 20)	4.6	96	6.5	48	40	248
Co-K	7.709	(25 15 1)	3.1	64	4.0	75	32	317
Ru-K	22.117	(38 10 16)	0.8	17	0.4	295	23	137
Re-L3	10.535	(38 0 12)	1.1	9	1.0	218	26	100
Os-L3	10.871	(15 25 29)	1.4	14	1.2	156	40	100
Ir-L3	11.215	(38 10 16)	1.5	32	1.3	143	46	186

2 keV.[9–12] The main strength in the performance of YB_{66} as a monochromator in the tender x-ray regime is twofold: (i) the absence of intrinsic absorption edges between 1 and 2 keV and (ii) the radiation damage resistance compared to other material candidates[32–34] for monochromatization, i.e., beryl, quartz, and InSb.

The exceptionally large lattice parameter of YB_{66} should lead in high density of reflections. By taking into account the atomic positions of all the 1584 boron and the 24 yttrium atoms in the unit cell, the lattice parameter in the measured temperature range, and the extracted Debye temperature, all reflections with a reflection coefficient more than 33% in exact backscattering geometry between 1 and 50 keV were calculated by the dynamical theory of diffraction and shown in Fig. 5. Two prominent features are seen in Fig. 5. On the one hand, an abrupt change in the reflectivity of backscattering reflections close to 17 keV is observed. Such an abrupt change is related with the x-ray absorption edge of Y, 24 atoms of which are located in the unit cell. On the other hand, the density of reflections across the full energy range is arguably impressive. For example, between 14.3 and 14.5 keV, 22 backscattering reflections at discrete energies with theoretical spectral reflectivity more than 33% are found. Notably, in the same energy range, only one backscattering reflection is found for Si and 13 backscattering reflections are found for Al_2O_3.[6]

The Debye temperature extracted in this study using three different experimental techniques is above 1000 K and shows a maximum temperature span around 20% from an average value extracted from the three experimentally obtained Debye temperatures. The reflection coefficient calculated using dynamical diffraction theory for all reflections in Fig. 5 using all three Debye temperatures varies only by around 5%. This practically indicates that an ultrahigh accuracy in the Debye temperature determination is not mandatory for x-ray optics applications.

Several reflections of YB_{66} in backscattering geometry exist that match the energy of x-ray absorption edges. Some possible reflections and their characteristics are given in Table II. The temperature at which these reflections meet the exact backscattering criterion appears also in Table II. The lowest temperature reported in Table II is 100 K. Thus, only a cryogenic system based on liquid nitrogen is required for achieving exact backscattering conditions for these reflections. The energy resolution provided by all reflections shown in Table II using a single YB_{66} crystal is in the meV range. A typical temperature to energy conversion factor, $\delta E/\delta T$, can be calculated by taking into account the x-ray energy and the thermal expansion coefficient at the temperature at which the reflection meets the backscattering criterion. A typical value of $\delta E/\delta T$ for the reflections included in Table II is $\sim$0.1 meV/mK. Thus, in order to carry out vibrational and/or magnetic spectroscopy, a temperature accuracy in the range of mK is required. Such a temperature accuracy is trivial for this kind of applications.[35]

The angular divergence of undulator sources at third generation synchrotron radiation storage rings is close to 10 μrad. The angular acceptance for the majority of exact backscattering reflections presented in Table II is above 10 μrad. As a result, at exact backscattering, only a slight collimation might be necessary for the (38 0 12) reflection pertinent to the Re-L3 edge. At this point, the reader should note that the angular acceptance is pretty much entirely determined practically by the deviation from backscattering.

The extinction length of the x-ray radiation for all reflection included in Table II is less than 300 μm, which means that even a 1 mm thick YB_{66} crystal is sufficiently thick and can easily be used for energies up to 22 keV. All in all, YB_{66} crystals have all potentials to be utilized in high-resolution monochromatization applications in the vicinity of x-ray edges. Such crystals are proven to have a decent quality for applications in the tender x-ray energy regime.[9,10] However, a thorough rocking curve imaging[36] or a backscattering topography[7] characterization on YB_{66} crystals may be useful in order to explore the quality of available YB_{66} crystals. Notably, because of the very large unit cell and the presence of high density of reflection multiple beam, x-ray diffraction might appear that could influence the spectral reflectivity of individual reflections, the obtained energy resolution, and the angular acceptance of the x-ray beam.[37] The density of x-ray reflections relevant to YB_{66} crystals might also be utilized for high and ultrahigh precision x-ray polarimetry applications[38,39] (scattering at a Bragg angle of 45°) provided that the multi-beam diffraction is not detrimental in such a case.

V. CONCLUSIONS

The crystal structure, the thermal expansion coefficient, and the stiffness of the YB_{66} unit cell are explored using both microscopic, i.e., powder and single crystal x-ray diffraction, inelastic x-ray scattering, and macroscopic, i.e., heat capacity, experimental methods. The information obtained was used to calculate the

11 July 2023 08:07:10

Published under an exclusive license by AIP Publishing

pertinent parameters of x-ray reflections in exact backscattering geometry between 1 and 50 keV in the context of dynamical diffraction theory. Specific reflections for meV resolution spectroscopy close to x-ray absorption edges are indicated and the relevant parameters, i.e., the expected energy resolution, the reflectivity, and the extinction length, are given.

ACKNOWLEDGMENTS

The synchrotron radiation facilities PETRA 3 and SPring-8 are acknowledged for provision of synchrotron radiation beamtime at P02, BL02B1 (proposal number: 2019A1174), and BL43LXU, respectively. D.B. would like to thank the Materials Dynamics Lab of the RIKEN SPring-8 Center for hosting and for providing access to resources pertinent to this study.

DATA AVAILABILITY

The data that support the findings of this study are available from the corresponding author upon reasonable request.

REFERENCES

[1]L. J. P. Ament, M. van Veenendaal, T. P. Devereaux, J. P. Hill, and J. van den Brink, "Resonant inelastic X-ray scattering studies of elementary excitations," Rev. Mod. Phys. **83**, 705–767 (2011).
[2]T. Ishikawa, "High-resolution X-ray optics for third-generation synchrotron radiation," J. Phys. D: Appl. Phys. **28**, A256–A261 (1995).
[3]J. P. Sutter, A. Baron, T. Ishikawa, and H. Yamazaki, "Examination of Bragg backscattering from crystalline quartz," J. Phys. Chem. Solids **66**, 2306–2309 (2005).
[4]I. Sergueev, H.-C. Wille, R. P. Hermann, D. Bessas, Yu. V. Shvyd'ko, M. Zajac, and R. Rüffer, "Milli-electronvolt monochromatization of hard X-rays with a sapphire backscattering monochromator," J. Synchrotron Radiat. **18**, 802–810 (2011).
[5]V. E. Asadchikov, A. V. Butashin, A. V. Buzmakov, A. N. Deryabin, V. M. Kanevsky, I. A. Prokhorov, B. S. Roshchin, Y. O. Volkov, D. A. Zolotov, A. Jafari, P. Alexeev, A. Cecilia, T. Baumbach, D. Bessas, A. N. Danilewsky, I. Sergueev, H.-C. Wille, and R. P. Hermann, "Single-crystal sapphire microstructure for high-resolution synchrotron X-ray monochromators," Cryst. Res. Technol. **51**, 290–298 (2016).
[6]Yu. V. Shvyd'ko, *X-ray Optics: High-Energy-Resolution Applications* (Springer, Berlin, 2004), Vol. 98.
[7]J. P. Sutter, A. Q. R. Baron, D. Miwa, Y. Nishino, K. Tamasaku, and T. Ishikawa, "Nearly perfect large-area quartz: 4 meV resolution for 10 keV photons over 10 cm^2," J. Synchrotron Radiat. **13**, 278–280 (2006).
[8]M. G. Hönnicke, X. Huang, C. Cusatis, C. N. Koditwuakku, and Y. Q. Cai, "High-quality quartz single crystals for high-energy-resolution inelastic X-ray scattering analyzers," J. Appl. Crystallogr. **46**, 939–944 (2013).
[9]M. Kitamura, H. Yoshikawa, T. Mochizuki, A. M. Vlaicu, A. Nisawa, N. Yagi, M. Okui, M. Kimura, T. Tanaka, and S. Fukushima, "Performance of YB_{66} double-crystal monochromator for dispersing synchrotron radiation at SPring-8," Nucl. Instrum. Methods Phys. Res., Sect. A **497**, 550–562 (2003a).
[10]A. D. Smith, B. C. Cowie, G. Sankar, and J. M. Thomas, "Use of YB_{66} as monochromator crystals for soft-energy EXAFS," J. Synchrotron Radiat. **5**, 716–718 (1998).
[11]J. Wong, Z. Rek, M. Rowen, T. Tanaka, F. Schäfers, B. Müller, G. George, I. Pickering, G. Via, B. DeVries, G. Brown, and M. Fröba, "New opportunities in 1–2 keV spectroscopy," Physica B **208**, 220 (1995).
[12]M. Kitamura, H. Yoshikawa, T. Tanaka, T. Mochizuki, A. Vlaicu, A. Nisawa, N. Yagi, M. Okui, M. Kimura, and S. Fukushima, "Non-existence of positive glitches in spectra using the YB_{66} double-crystal monochromator of BL15XU at SPring-8," J. Synchrotron Radiat. **10**, 310–312 (2003b).
[13]T. Tanaka, Z. Rek, J. Wong, and M. Rowen, "FZ crystal growth of monochromator-grade YB_{66} single crystals as guided by topographic and double-crystal diffraction characterization," J. Cryst. Growth **192**, 141–151 (1998).
[14]T. Tanaka, S. Otani, and Y. Ishizawa, "Growth of high quality single crystals of YB_{66}," J. Cryst. Growth **99**, 994–997 (1990).
[15]H. Suzuki, A. Inaba, and C. Meingast, "Accurate heat capacity data at phase transitions from relaxation calorimetry," Cryogenics **50**, 693–699 (2010).
[16]QD-PPMS, "Heat Capacity Application Note" (2002).
[17]A. Q. R. Baron, "Introduction to high-resolution inelastic X-Ray scattering," arXiv:1504.01098 cond-mat.mtrl-sci (2020).
[18]A. Q. R. Baron, *Introduction to High-Resolution Inelastic X-Ray Scattering* (Springer International Publishing, 2016), pp. 1643–1757.
[19]A. Q. R. Baron, "Status of the RIKEN quantum nanodynamics beamline (BL43LXU): The next generation for inelastic X-ray scattering," SPring-8 Information Newsletter **15**, 14 (2010).
[20]F. Sayetat, P. Fertey, and M. Kessler, "An easy method for the determination of Debye temperature from thermal expansion analyses," J. Appl. Crystallogr. **31**, 121–127 (1998).
[21]R. P. Hermann, F. Grandjean, and G. J. Long, "Einstein oscillators that impede thermal transport," Am. J. Phys. **73**, 110–118 (2005).
[22]H. Fukui, T. Katsura, T. Kuribayashi, T. Matsuzaki, A. Yoneda, E. Ito, Y. Kudoh, S. Tsutsui, and A. Q. R. Baron, "Precise determination of elastic constants by high-resolution inelastic X-ray scattering," J. Synchrotron Radiat. **15**, 618–623 (2008).
[23]A. U. Seybolt, Trans. Am. Soc. Met. **52**, 971 (1960).
[24]M. A. Hossain, I. Tanaka, T. Tanaka, A. U. Khan, and T. Mori, "YB_{48} the metal rich boundary of YB_{66}; crystal growth and thermoelectric properties," J. Phys. Chem. Solids **87**, 221–227 (2015).
[25]S. M. Richards and J. S. Kaspar, "The crystal structure of YB_{66}," Acta Crystallogr., Sect. B: Struct. Sci. **25**, 237–251 (1969).
[26]I. Higashi, K. Kobayashi, T. Tanaka, and Y. Ishizawa, "Structure refinement of YB_{62} and YB_{56} of the YB_{66}-type structure," J. Solid State Chem. **133**, 16–20 (1997).
[27]J. Wong, T. Tanaka, M. Rowen, F. Schäfers, B. R. Müller, and Z. U. Rek, "YB_{66} a new soft x-ray monochromator for synchrotron radiation," J. Synchrotron Radiat. **6**, 1086–1095 (1999).
[28]F. C. Nix and D. MacNair, "The thermal expansion of pure metals: Copper, gold, aluminum, nickel, and iron," Phys. Rev. **60**, 597–605 (1941).
[29]M. Beekman, D. T. Morelli, and G. S. Nolas, "Better thermoelectrics through glass-like crystals," Nat. Mater. **14**, 1182–1185 (2015).
[30]D. Oliver and G. D. Brower, "Growth of single crystal YB_{66} from the melt," J. Cryst. Growth **11**, 185–190 (1971).
[31]F. Herbstein, "Methods of measuring Debye temperatures and comparison of results for some cubic crystals," Adv. Phys. **10**, 313–355 (1961).
[32]B. Yang, F. Middleton, B. Olsson, G. Bancroft, J. Chen, T. Sham, K. Tan, and D. Wallace, "The design and performance of a soft X-ray double crystal monochromator beamline at Aladdin," Nucl. Instrum. Methods Phys. Res., Sect. A **316**, 422–436 (1992).
[33]M. D. Roper, P. A. Buksh, I. W. Kirkman, G. van der Laan, H. A. Padmore, and A. D. Smith, "Performance of the Daresbury synchrotron radiation source soft X-ray double-crystal monochromator," Rev. Sci. Instrum. **63**, 1322–1325 (1992).
[34]A. A. MacDowell, J. B. West, G. N. Greaves, and G. Van der Laan, "Monochromator and beamline for soft X-ray studies in the photon energy range 500 eV–5 keV," Rev. Sci. Instrum. **59**, 843–852 (1988).
[35]P. Alexeev, V. Asadchikov, D. Bessas, A. Butashin, A. Deryabin, F.-U. Dill, A. Ehnes, M. Herlitschke, R. P. Hermann, A. Jafari, I. Prokhorov, B. Roshchin, R. Röhlsberger, K. Schlage, I. Sergueev, A. Siemens, and H.-C. Wille,

11 July 2023 08:07:10

Published under an exclusive license by AIP Publishing

"The sapphire backscattering monochromator at the dynamics beamline P01 of PETRA III," Hyperfine Interact. **237**, 59 (2016).
[36]A. Jafari, I. Sergueev, D. Bessas, B. Klobes, B. S. Roschin, V. E. Asadchikov, P. Alexeev, J. Härtwig, A. I. Chumakov, H.-C. Wille, and R. P. Hermann, "Rocking curve imaging of high quality sapphire crystals in backscattering geometry," J. Appl. Phys. **121**, 044901 (2017).
[37]R. Colella, "Multiple diffraction of x-rays and the phase problem. Computational procedures and comparison with experiment," Acta Crystallogr., Sect. A **30**, 413–423 (1974).
[38]B. Marx, K. S. Schulze, I. Uschmann, T. Kämpfer, R. Lötzsch, O. Wehrhan, W. Wagner, C. Detlefs, T. Roth, J. Härtwig, E. Förster, T. Stöhlker, and G. G. Paulus, "High-precision x-ray polarimetry," Phys. Rev. Lett. **110**, 254801 (2013).
[39]H. Bernhardt, A. T. Schmitt, B. Grabiger, B. Marx-Glowna, R. Loetzsch, H.-C. Wille, D. Bessas, A. I. Chumakov, R. Rüffer, R. Röhlsberger, T. Stöhlker, I. Uschmann, G. G. Paulus, and K. S. Schulze, "Ultra-high precision x-ray polarimetry with artificial diamond channel cuts at the beam divergence limit," Phys. Rev. Res. **2**, 023365 (2020).

11 July 2023 08:07:10

Published under an exclusive license by AIP Publishing